



Proceedings of 36th International Conference on Ground Control in Mining (China · 2017)

—The Theory and Technical Progress on Ground Control in Mining

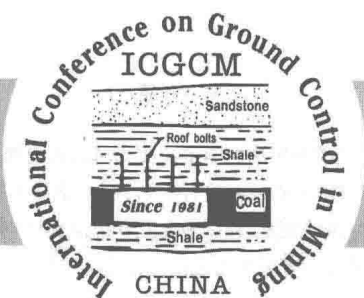
Editor-in-Chief: Yuan Liang Syd S.Peng

Associate Editor-in-Chief: Shi Biming Zhao Guangming

Zhang Xiangyang Yang Ke

非外借

China University of Mining and Technology Press



Proceedings of 36th International Conference on Ground Control in Mining (China· 2017)

—The Theory and Technical Progress on Ground Control in Mining

Editor-in-Chief: Yuan Liang Syd S.Peng

**Associate Editor-in-Chief: Shi Biming Zhao Guangming
Zhang Xiangyang Yang Ke**

China University of Mining and Technology Press

内 容 简 介

本书收录了国际与国内煤矿开采岩层控制领域的学术论文 63 篇,集中展示了国际采矿岩层控制领域近年来的发展方向与技术创新。主要议题包括千米深井安全高效开采、深部岩石力学与工程应用、采场岩层控制理论与技术、坚硬顶板岩层控制理论与技术、巷道围岩控制与防治技术、冲击地压及其防治理论与技术、煤与瓦斯共采理论与技术、大倾角煤层开采矿压控制理论与技术、煤层群协调开采矿压控制理论与技术、开采沉陷控制理论与技术、智能岩层控制、矿山灾害防治、与采矿岩层控制相关的主题等。

本书可供从事煤矿开采方面科研、设计、工程技术及管理人员阅读参考,也可供高等院校矿业工程研究领域师生参考。

图书在版编目(CIP)数据

煤矿岩层控制理论与技术进展:36 届国际采矿岩层控制会议(中国·2017)论文集=The Theory and Technical Progress on Ground Control in Mining:Proceedings of 36th International Conference on Ground Control in Mining (China·2017).下册:英文/袁亮,(美)彭赐灯(Syd S. Peng)主编.—徐州:中国矿业大学出版社,2017.9

ISBN 978-7-5646-3642-5

I. ①煤… II. ①袁… ②彭… III. ①煤矿开采—岩层控制—文集—英文 IV. ①TD325-53

中国版本图书馆 CIP 数据核字(2017)第 238628 号

- 书 名 Proceedings of 36th International Conference on Ground Control in Mining(China·2017)
—The Theory and Technical Progress on Ground Control in Mining
- 主 编 Yuan Liang [美]Syd S. Peng
- 责任编辑 王美柱
- 责任校对 仓小金
- 出版发行 中国矿业大学出版社有限责任公司
(江苏省徐州市解放南路 邮编 221008)
- 营销热线 (0516)83885307 83884995
- 出版服务 (0516)83885767 83884920
- 网 址 <http://www.cumtp.com> E-mail: cumtpvip@cumtp.com
- 印 刷 江苏淮阴新华印刷厂
- 开 本 787×1092 1/16 本册印张 13.5 本册字数 354 千字
- 版次印次 2017 年 9 月第 1 版 2017 年 9 月第 1 次印刷
- 总 定 价 158.00 元(上、下册)
- (图书出现印装质量问题,本社负责调换)

Academic Committee

Chairmen:

Syd S. Peng

Academician of American Academy of Engineering, USA

Yuan Liang

Academician of Chinese Academy of Engineering, China

Peng Suping

Academician of Chinese Academy of Engineering, China

Cai Meifeng

Academician of Chinese Academy of Engineering, China

Gu Dazhao

Academician of Chinese Academy of Engineering, China

Jin Zhixin

Academician of Chinese Academy of Engineering, China

Ling Wen

Academician of Chinese Academy of Engineering, China

Wu Qiang

Academician of Chinese Academy of Engineering, China

Kang Hongpu

Academician of Chinese Academy of Engineering, China

Liu feng

Professor

Guo Yongcun

Professor

Wang Qidong

Professor

Feng Xiating

Professor

Vice-chairmen(in Chinese alphabet order) :

Cheng Hua	Chi Xiuwen	Feng Tao	Hao Chuanbo
Hua Xinzhu	Jiang Deyi	Li Shugang	Li Xibing
Liang Bing	Liang Weiguo	Liu Quansheng	Meng Xiangrui
Qi Qingxin	Shi Biming	Tang Yongzhi	Wang Jiachen
Wu Aixiang	Yang Renshu	Zhang Dongsheng	Zhang Nong
Zhou Ying	Zhu Wancheng	Zhu Wangxi	

Members(in Chinese alphabet order) :

Chang Jucai	Cheng Yunhai	Feng Guorui	Gao Mingzhong
Gao Zhaoning	Guo Wenbing	Hu Youbiao	Ji Hongguang
Jing Laiwang	Li Yingming	Liu Hongtao	Ma Qinyong
Min Fanfei	Tan Yunliang	Tu Min	Wang Lei
Wang Weijun	Wu Yongping	Yang Ke	Yuan Shujie
Zha Wenhua	Zhang Guohua	Zhang Hongwei	Zhang Jixiong
Zhao Guangming	Zhou Keping	Zhu Jinbo	

Organizing Committee

Chairmen:

Yuan Liang Syd S. Peng

Vice-chairmen:

Hua Xinzhu Min Fanfei Shi Biming

Secretary general:

Zhao Guangming

Secretary:

Zhang Xiangyang

Contents

Numerical simulation of strength degradation in creep failure of laboratory rock specimens	XUE Yu-ting, MISHRA Brijes (1)
Study on mechanical properties of coal measures rocks with triaxial compression in Panji deep exploration	SHEN Shu-hao, WU Ji-wen, ZHAI Xiao-rong, et al (9)
Influence of storage period and water content of dry-mixed materials on dynamic compressive strength for ready-mixed shrinkage-compensating concrete	MA Qin-yong, ZHANG Yang-yang, MA Dong-dong (16)
Mechanism and experiment investigation on the formation of hydro-fracture system by fracturing through the interface of large-size coal-rock	WU Peng-fei, LIANG Wei-guo, LIAN Hao-jie, et al (24)
Study on coupling evolution law of hydraulic cracks and stress field in hard roof	DENG Guang-zhe, XU Dong (40)
Analysis of creep deformation and failure characteristics of siltstone specimens under shock disturbance	LIU Xiao-lin, SU Rong-hua, LIU Zhen-yang, et al (55)
Prediction of the roof weighting using the parameters back-analysis method combined with genetic algorithms	CHEN Yue-du, LIANG Wei-guo, YANG Jian-feng, et al (61)
Actual measurement and analysis on deformation characteristics of fault structure under mining condition	ZHANG Ping-song, LU Hai-feng, HAN Bi-wu, et al (76)
Study on strata behavior and variation law of bolt shaft force of fully mechanized coal mining face under fault	SHI Hao, ZHANG Hou-quan (85)
Experimental investigation on anchorage performance of bolts with different structures	ZHAO Xiang-zhuo, WU Tao, ZHANG Hong-wei, et al (92)
Test study on attenuation characteristics of anchoring force for bolt hole reaming anchorage in soft coal and rock mass	ZHANG Hui, LI Guo-sheng, Jiang Shuai-qi (104)
Analysis of fracture structure impact on rockburst	LAN Tian-wei, ZHANG Hong-wei, HAN Jun, et al (114)
Investigations into the impacts on coal-rock body gas pressure release exercised by selection of different mining parameters for soft rock protective seam	ZHAO Guang-ming, MENG Xiang-rui, CHENG Xiang, et al (121)

- Experimental study on the relation between initial gas discharge and
outburst intensity *YANG Ding-ding, JIANG Cheng-lin, Tang Jun, et al* (139)
- Fully-mechanized top caving technology of longwall working face with variable dip
angle in steeply inclined extra thick seam
..... *WANG Hong-wei, WU Yong-ping, XIE Pan-shi, et al* (150)
- The classification of shallow buried close seams group and support resistance
determination of stope *HUANG Qing-xiang, CAO Jian, HE Yan-peng* (160)
- Joint detection while drilling by monitoring roof bolter drilling parameters application
in underground mining and tunneling
..... *Wenpeng Liu, Jamal Rostami, Joe McQuerrey* (175)
- Implementation of the first large diameter lifesaving vertical surface hole
in China *TANG Yong-zhi, ZHAO Jun-feng, DING Tong-fu, et al* (187)
- Influence of interaction of groundwater with clay on the premature failure
of rockbolts *S. Wu, L. Saad, H. L. Ramandi, et al* (196)

Numerical simulation of strength degradation in creep failure of laboratory rock specimens

XUE Yu-ting, MISHRA Brijes

(*Department of Mining Engineering, West Virginia University, Morgantown, WV 26505, USA*)

Abstract: Failure of rock specimen in creep tests are known to occur at stresses that are lower than the strength of the intact rock. The time to reach failure depends on the stress levels. Failure in rock specimens occur due to the strength degradation induced by the viscous deformation. In this paper, the parameter-effective viscous strain was introduced to simulate the strength degradation induced during creep. The model was implemented in the three dimensional distinct element code(3DEC). The viscous behavior of rock was characterized by Burgers model and the relation between the effective viscous strain and strength value was determined from laboratory creep test. During creep simulation, the real-time strength value was determined from the effective viscous strain calculated at each time-step in 3DEC. Result from the simulation effort shows that the new model can reproduce the failure of rock specimens undergoing unconfined creep test.

Keywords: creep; strength degradation; failure; numerical simulation

Introduction

Roof fall is always a major safety hazard in underground coal mines. Field observation demonstrates that competent roofs of coal mines do not fail immediately after the excavation but sometime later, depending on various factors (Dolinar et al., 2000; Ray, 2009). The process of massive failure begins with localized failure that gradually progresses along the mine entry, and when the failure reaches the competent, overlying strata, the entire roof rock collapses, exposing the overlying strata. This involves time-dependent deformation and failure. For the time-dependent deformation, laboratory creep tests can be conducted to determine the time-dependent parameters for a creep model. Mohr-Coulomb failure criterion can be combined with a creep model to account for the failure under creep condition. The viscoelastic plastic model, combining Burgers creep model and Mohr-Coulomb failure criterion, is referred as *cvisous* model in 3DEC (Itasca 2012), which was used to simulate an unconfined creep test. A constant stress of ninety-eight percent of the strength was applied on the top of the simulated specimen. The model was run to equilibrium condition first to obtain the elastic solution. The instantaneous elastic strain was 4.35×10^{-4} . Creep simulation was then activated to run for a time equivalent to 2×10^6 seconds (555.6 hours). As shown in Fig. 1, the specimen deforms without failure with the axial viscous strain is almost seventeen times as the instantaneous

elastic strain. However, this is not the situation in laboratory tests.

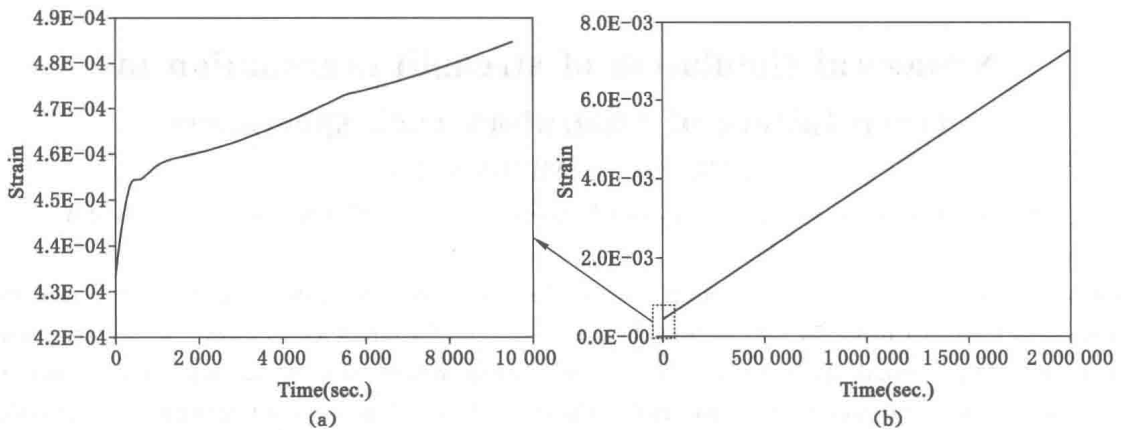


Fig. 1 Stress-strain curve for the simulated unconfined creep test with Burgers model and Mohr-Coulomb criterion

Failure of rock specimen in creep tests are known to occur at stresses that are lower than the strength of the intact rock (Wawersik and Brown, 1971; Baud and Meredith, 1997; Rinne, 2008), indicating that the rock strength degrades during the creep test. The acoustic emission output from triaxial creep test on sandstone shows that the time-dependent cracking plays the major role during the secondary stage of creep (Baud and Meredith, 1997). Rinne (2008) adopted subcritical crack theory to simulate the delayed failure of a loaded rock and the result demonstrates that the slow time-dependent fracturing process may lead to a sudden unstable failure event. Lin et al. (2009) carried out a series of constant loading tests with acoustic emission monitoring and the source location analysis reproduced the progressive damage process during the test. These demonstrate that subcritical cracks can still propagate during creep test and therefore deteriorate the rock specimens. If the strength degradation caused by viscous deformation is not considered, the strength remains constant during creep test. The applied stress is constant and is lower than the rock strength and therefore, the specimen deforms without failure.

Various methods have been proposed to consider the strength degradation induced by viscous deformation. Wawersik and Brown (1971) used maximum creep strain as failure criterion, which could be obtained from the strain between the ascending and descending parts of the complete quasi-static stress-strain curve. The results of uniaxial compression creep tests (Kranz and Scholz, 1977) showed that the inelastic volumetric strain at the onset of tertiary creep was nearly constant, independent of stress level and related to fracture strength and rock type. Malan (1999) also derived a time-dependent Mohr-Coulomb failure criterion, where the cohesion was considered to degrade with time and the degradation rate depended on the distance between the stress state and the residual strength. Fakhimi (1994) proposed a model to investigate the stand-up time of underground excavations where the strength degraded exponentially with effective viscous strain.

Similar to the effective shear plastic strain in strain-softening model, the effective viscous strain is a parameter qualifying the damage induced by the viscous behavior and can be related to the rock strength. With such a parameter, the strength degradation caused by viscous deformation can be considered for complicated stress condition and be used in numerical simulation. The concept of effective viscous strain was used in this paper to quantify the damage induced by viscous strain and to control the strength degradation with viscous strain.

1 Effective viscous strain for burgers materials

Burgers model is widely used to represent the creep behavior of rocks (Price, 1964; Fakhimi and Fairhurst, 1994; Ghorbani and Sharifzadeh, 2009). Burgers model for unconfined creep condition is shown in Eq. 1, where K and E_m are the bulk and shear modulus while η_m , E_k , and η_k are the creep or time-dependent parameters shown in Fig. 2. In Eq. 1, the first term of the right side is the volumetric strain and the left three terms represent the deviatoric strain. Therefore, the material behaves as an elastic body under hydrostatic compression and as a Burgers material under deviatoric stress condition (Goodman, 1989).

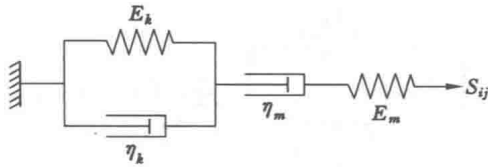


Fig. 2 Schematic of Burgers model

$$\epsilon = \frac{\sigma}{9K} + \frac{\sigma}{3E_m} + \frac{\sigma}{3\eta_m}t + \frac{\sigma}{3E_k} \left[1 - \exp\left(\frac{-E_k t}{\eta_k}\right) \right] \quad (1)$$

It can be found from Eq. 1 that the first two terms of the right side describe the time-independent response of the axial strain to axial stress and the left two terms represent the time-dependent behavior. The relation between the viscous strain and time in axial direction can then be described as,

$$\epsilon^v = \frac{\sigma}{3\eta_m}t + \frac{\sigma}{3E_k} \left[1 - \exp\left(\frac{-E_k t}{\eta_k}\right) \right] \quad (2)$$

The strength degradation parameter κ^v is introduced to control the time-dependent strength degradation. It is a measure of the second invariant of the viscous strain, given as,

$$\kappa^v = \sqrt{\frac{2}{3} \epsilon_{ij}^v \epsilon_{ij}^v} \quad (3)$$

Where, ϵ_{ij}^v represents the viscous strain in three-dimensional condition. For unconfined condition, the strength degradation can be derived as,

$$\kappa^v = \frac{\sqrt{3}}{2} |\epsilon^v| \quad (4)$$

The strength degradation parameters can be calculated with the axial strain during an unconfined creep test. At the same time, the relation between κ^v and strength value can be determined if the unconfined creep test continues until the specimen fails. Under this circumstance, the constant stress applied to the specimen is the strength value. Due to the viscous deformation, the rock strength is decreased from the original value to the stress value of the creep test. Therefore, the strength value for one specimen with specific effective viscous strain values can be obtained.

2 Calculation of effective viscous strain in 3DEC

The relation between the strength degradation parameters and strength value, obtained from creep tests, can be input into 3DEC code to control the strength degradation during time-dependent simulations. At each time-step, the accumulated effective viscous strain can be calculated and then is used to update the strength value based on the strength degradation relation provided by users. The calculation of effective viscous strain in 3DEC is summarized in this section.

Only the viscous part of Burgers model is considered here, as shown in Fig. 3. For the Maxwell unit, we have,

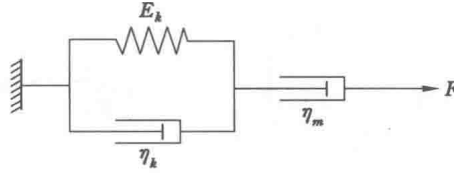


Fig. 3 Schematic of viscous part in Burgers model

$$\dot{u}_m = \frac{\bar{F}}{\eta_m} \quad (5)$$

Where, \dot{u}_m is the strain rate of the Maxwell unit and \bar{F} corresponds to the mean values of F over the time-step with the format of Eq. 6. The superscripts n and 0 denote the new and old values, respectively.

$$\bar{F} = \frac{F^n + F^0}{2} \quad (6)$$

Writing Eq. 5 in finite-difference form,

$$u_m^n = u_m^0 + \frac{F^n + F^0}{2 \eta_m} \Delta t \quad (7)$$

For the Kelvin part (Itasca, 2014), we have,

$$u_k^n = \frac{1}{A} \left[B u_k^0 + (F^n + F^0) \frac{\Delta t}{2 \eta_k} \right] \quad (8)$$

Where

$$A = 1 + \frac{E_m \Delta t}{2 \eta_k} \quad (9)$$

$$B = 1 - \frac{E_m \Delta t}{2 \eta_k} \quad (10)$$

At each time-step, the new viscous strain can be calculated by adding up the Maxwell viscous strain in Eq. 7 and the Kelvin strain in Eq. 8. For three-dimensional condition, the symbols S_{ij} is used to represent the deviatoric stress tensor and ϵ_{ij}^v represents the viscous strain tensor. The superscripts k, m , and p are used to represent the contributions of the Kelvin, Maxwell and plastic components of stresses and strains, respectively.

$$e_{ij}^{m,n} = e_{ij}^{m,o} + \frac{\Delta t}{4 \eta^m} (S_{ij}^n + S_{ij}^o) \quad (11)$$

$$e_{ij}^{k,n} = \frac{1}{A} \left[B e_{ij}^{k,o} + \frac{\Delta t}{4 \eta^k} (S_{ij}^n + S_{ij}^o) \right] \quad (12)$$

The viscous strain tensor can be further calculated as,

$$e_{ij}^v = e_{ij}^m + e_{ij}^k \quad (13)$$

Which can be substituted into Eq. 3 to calculate the accumulated effective viscous strain at each time step.

3 Numerical simulation of the creep failure of laboratory rock specimens

A series of laboratory unconfined creep tests were simulated to verify the new model. Burgers creep model was used to describe the time-dependent behaviors and Mohr-Coulomb criterion was used as the failure criterion. The strength degradation relation was given by the relation between friction angle and the effective viscous strain, as shown in Fig. 4, which can be input into 3DEC code as a table, similar to the strain-softening model. The resulted strength degradation relation is shown in Fig. 5. The effective viscous strain gradually accumulates with time during a creep test, leading to decreasing strength value. Specimen failure occurs when the strength value reduces to the value equaling to applied constant stress.

The simulation results demonstrate that the model can reproduce the creep failure of laboratory specimens. It can be observed from Fig. 6 that the simulated specimens show typical creep behavior where the creep curves have three stages-primary, secondary and tertiary. The accelerating strain rate after the secondary stage indicates the failure of the specimen. Therefore, the simulated specimens fail after sometime when the creep test starts. However, there are three specimens keeping deforming without failure. This is because of the provided strength degradation relation. As shown in Fig. 5, the strength degradation relation becomes a horizontal line when the strength reduces to 23.81 MPa, indicating that this is the lower bound for strength degradation. If the applied stress is below this value, the specimen keeps deforming without failure. In addition, it can be found from Fig. 6 that the time to failure depends on applied constant stress. It takes longer time to fail the specimen if the applied constant stress is lower. The relation between time to failure and the applied stress is plotted in Fig. 7. It shows similar trend as the strength degradation relation in Fig. 5.

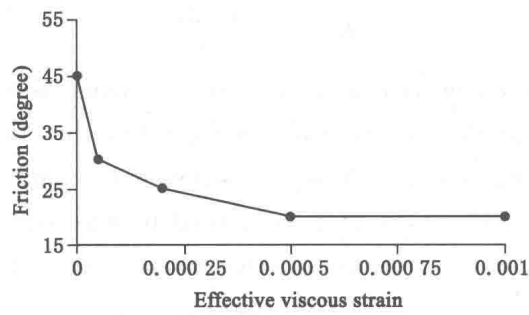


Fig. 4 Relation between friction and effective viscous strain used in the simulation

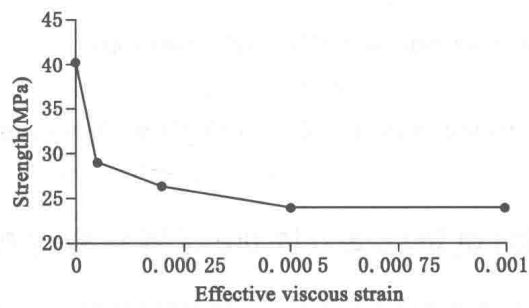


Fig. 5 Strength degradation relation

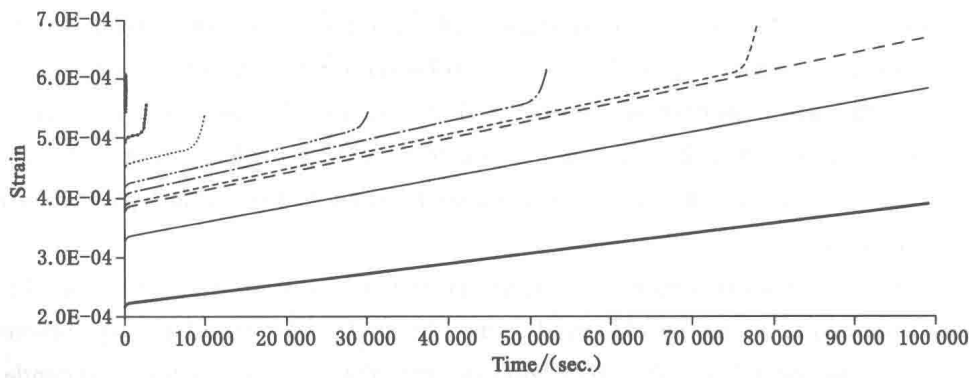


Fig. 6 Results of simulated creep tests with strength degradation

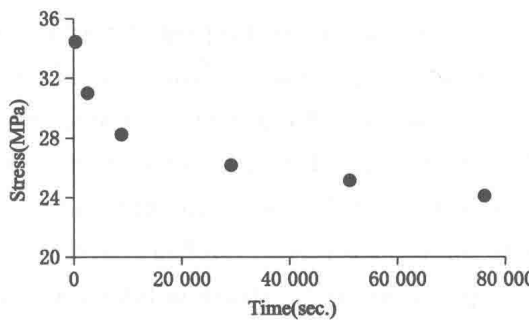


Fig. 7 Time to failure with different constant stresses

4 Conclusions

Failure of rock specimen in creep tests are known to occur at stresses that are lower than the strength of the intact rock. Due to subcritical crack propagation and other mechanisms, the viscous deformation introduces damage to the rock specimens and therefore induces strength degradation. However, the viscoelastic-plastic model, with the viscoelastic model and the failure criterion, cannot reproduce the creep failure observed in laboratory tests. The parameter of effective viscous strain was introduced in this paper to quantify the damage induced by viscous deformation and to control the strength degradation in numerical simulation with 3DEC. The relation between strength values and the effective viscous strains can be determined from laboratory creep tests and be input into 3DEC code as a table. During numerical simulation, the strength value can be updated at each time-step after the accumulated effective viscous strain is calculated. The simulation results demonstrate that the new model can reproduce the failure of rock specimens undergoing unconfined creep test.

References

- [1] Baud P, Meredith P G. Damage accumulation during triaxial creep of darley dale sandstone from pore volumetry and acoustic emission[J]. *Int. J. Rock Mech. Min. Sci.*, 1997(34):24-31.
- [2] Dolinar D R, Mucho T P, Oyler D C, et al. Utilizing the “advance and relieve” method to reduce horizontal stress affects on the mine roof, a case study [C]. In: 19th Conference on Ground Control in Mining, 2000.
- [3] Fakhimi A, Fairhurst C. A model for the time-dependent behavior of rock[J]. *Int. J. Rock Mech. Min. Sci. Geomech. Abstr.*, 1994(31):117-126.
- [4] Ghorbani M, Sharifzadeh M. Long term stability assessment of Siah Bisheh powerhouse cavern based on displacement back analysis method[J]. *Tunn. Undergr. Sp. Technol.*, 2009(24):574-583.
- [5] Goodman R E. Introduction to rock mechanics-second edition [M]. New York: Wiley, 1989.
- [6] Itasca. 3DEC-Three-dimensional distinct element code version 5. 0 user’ s manual [R]. 2012.
- [7] Kranz R L, Scholz C H. Critical dilatant volume of rocks at the onset of tertiary creep [J]. *J. Geophys. Res.*, 1997(82):4892-4895.
- [8] Lin Q X, Liu Y M, Tham L G, et al. Time-dependent strength degradation of granite [J]. *Int. J. Rock Mech. Min. Sci.*, 2009(46):1103-1114.
- [9] Malan D F. Time-dependent behaviour of deep level tabular excavations in hard rock [J]. *Rock Mech. Rock Eng.*, 1999(32):123-155.
- [10] Price N J. A study of the time-strain behavior of coal-measure rocks[J]. *Int. J. Rock*

Mech. Min. Sci. ,1964(1):277-303.

- [11] Ray A K. Influence of cutting sequence and time effects on cutters and roof falls in underground coal mine-numerical approach[D]. West Virginia University,2009.
- [12] Rinne M. Fracture mechanics and subcritical crack growth approach to model time-dependent failure in brittle rock[J]. Helsinki University of Technology,2008.
- [13] Wawersik W R,Brown W S. Creep fracture in rock in uniaxial compression[C]. Salt Lake City; Utah,USA,1971.

Study on mechanical properties of coal measures rocks with triaxial compression in Panji deep exploration

SHEN Shu-hao¹, WU Ji-wen¹, ZHAI Xiao-rong¹, SHI Wen-bao²

(1. *School of Earth and Environment, Anhui University of Science and Technology, Huainan 232001, China;*

2. *Anhui Province Key Laboratory of Mining Response and Disaster Prevention and Control in Deep Coal Mine, Huainan 232001, China)*

Abstract: Taking the deep exploration area in Panji of Huainan as an example, the distribution characteristics of deep geological storage conditions for the coal measures rocks were comprehensively determined. In the variation range of measured in-situ stress condition, the strength characteristics and deformation properties of coal measures rocks were studied by rock triaxial compression test system indoor. The coal measures rocks include 6 kinds of lithology: gritstone, medium sandstone, fine sandstone, siltstone, mudstone and limestone. The results showed that the high lateral pressure plays a important role in the mechanical properties of coal measures rocks. According to the analysis of the similarities and differences of each lithology rocks, the strength and deformation of coal measures rocks under the high stress field are controlled by the lateral pressure control greater than the influence of lithology. Results canbe applied to the deep engineering disaster prevention and stability evaluation of surrounding rocks.

Keywords: coal measures rocks; triaxial compression; mechanical properties; deep exploration

Introduction

Geological prospecting work has achieved remarkable results, the exploration and exploitation of coal resources gradually extend to the deep in recent years. The accurate rock mechanics parameters are needed for the evaluation of geological conditions in major engineering exploration phase and the later design, the basic research on the mechanical properties of rock under deep in-situ stress field is the primary demand for ensure the construction of the mine, efficient mining and the prevention of major engineering geological disasters (He and Zhu, 2016; Xie et al., 2015). At present, the theory and technology of rock indoor test under high pressures in stress field have developed rapidly, that accelerated the relationship between strength and deformation characteristics of rock and lateral pressure research (You, 2014; Lai, 2009).

Over years, triaxial compression tests have focused on homogeneous rocks such as

Supported by the National Natural Science Foundation of China (41272278), Anhui provincial natural science research projects in Colleges and Universities (KJ2017A073), Anhui provincial geological prospecting fund third projects (sequel) (2013-3-18).

Tel: 86-15212671330, E-mail: shuhao2013@126.com.